Characterizing aerosol from space with the MODerate resolution Imaging Spectroradiometer (MODIS) on the Terra and Aqua satellites

Robert C. Levy, Lorraine A. Remer, Yingxi Shi, Richard G. Kleidman, and the Dark Target team

Abstract

Aerosols, the small, suspended liquid and solid particles in the atmosphere, have myriad effects on climate, weather, and air quality. When the NASA Earth-Observing System's (EOS) Terra and Aqua satellites launched in 1999 and 2002, they each included many advanced sensors that have been used for aerosol research. In particular, the MODerate-resolution Imaging Spectroradiometer (MODIS) deployed on both satellites, has provided key data relating to aerosol loading and relative aerosol type on the global scale. Three different algorithms, known as "Dark Target", "Deep Blue" and "MAIAC", use different subsets of MODIS measurements and different assumptions to create various products such as Aerosol Optical Depth (AOD), fine mode fraction (FMF) and single scattering albedo (SSA). Although all three derive AOD in cloud-free conditions, each algorithm has different strengths and weaknesses in different areas of the globe and under different conditions. Here, we provide a short summary of each algorithm, description of products, and basic information about downloading and using the products. We also provide some examples of how MODIS aerosol products are used. Finally, we add a quick discussion about how these algorithms and products will continue after MODIS leaves orbit.

1. Aerosol Properties

Aerosols are small (order <0.1 to >10 μm) suspended liquid and solid particles in the atmosphere, known in the air pollution community as Particulate Matter (PM). Arising from a combination of mechanical and chemical processes, aerosol "types" such as dust, smoke, salt, and industrial pollution have all sorts of impacts in climate and air pollution. By reflecting and absorbing solar radiation, aerosols lead to haze which affects visibility. For the same reason, they play significant roles in Earth's energy balance [1] [2] and tend to offset warming by greenhouse gases. Aerosols impact cloud through microphysical processes such as droplet formation and modify the environment in which clouds develop [1] [2] [3], thus leading to an indirect climate effect [4]. Finally, when concentrated near the surface, aerosols (as particulate matter, PM) have been identified as one of the leading factors in the global burden of disease [5]. Particles having aerodynamic diameters less than 2.5 μm (known as PM2.5) are known to be hazardous to human health.

Aerosols include particles arising from physical, chemical and biological processes. Examples include dust and salts lifted from the land and ocean surface, smoke from biomass burning and haze from industrial and natural processes. Larger than molecules and smaller than cloud droplets, we are primarily interested in the size range between 0.1 and 10 μm. In nature, aerosols are not of uniform size, but rather participate within a *size distribution*, which can

often be approximated by one or more *lognormal* modes, each having a characteristic mean and standard deviation of particle radius (or diameter). Generally, dust and sea-salt particles are larger than urban/industrial and smoke. Another important aspect is the particle *shape*. Aerosols from industrial sources tend to be approximately spherical, whereas sea-salt or dust particles are non-spherical and appear as crystals or tiny rocks. Finally, there is the chemical composition, which manifests itself as a spectrally-dependent complex refractive index (function of wavelength). The combination of aerosol size, shape, and refractive index we refer to as the *aerosol particle properties*. Note that as aerosols are transported, or are further involved in chemical and physical processes (e.g. processing in clouds or precipitation), these properties may change. A collection of particles will *scatter* and *absorb* radiation, the sum of which is known as *extinction.* The ratio of scattering to extinction, known as the single scattering albedo (SSA), ranges between 0.8 and 1.0 for most aerosols in visible wavelengths.

Light scattering efficiency (scattering per particle) is largest when particles are of similar size (radius) to the wavelength. Smaller-sized *fine* particles with radius r<<1 μm efficiently scatter visible-wavelength radiation (e.g. 0.4 – 0.7 μm), whereas larger-sized *coarse* particles (r >1 μm) are more efficient in scattering shortwave infrared (e.g., ~2 μm). Thus, remote sensing in multiple wavelengths helps infer relative aerosol size. Note the size-overlap with our "fine" particles and PM2.5 (diameter < 2.5 μm).

We can measure aerosol loading by the unitless *aerosol optical depth* (AOD or τ), a wavelength dependent (function of λ) optical measurement. AOD is the integral of the aerosol extinction coefficient β_λ (units of m^{-1}) over the vertical path (*z*) from the surface (SFC) to the top of the atmosphere (TOA), as shown in Eq. (1).

$$\tau_\lambda = \int_{SFC}^{TOA} \beta_\lambda(z)dz \qquad (1)$$

One should note that the term *optical depth* generally represents not only the aerosol portion, but also contributions from molecular scattering (Rayleigh) and absorption from trace gases. However, if we can observe in atmospheric "windows" (wavelengths with negligible or correctable gas absorptions), and we can accurately estimate molecular scattering as a function of surface pressure and latitude, then we can determine the aerosol portion of the total optical depth (AOD).

The most direct measure of AOD is by ground-based sunphotometer, which is a columnated radiometer that observes exactly only the sun's disk. By measuring the incoming radiance in a window wavelength, λ, along with known values of the incoming solar radiance at the TOA, one can accurately determine the AOD via the Beer-Bouger equation. A federated network of sunphotometers known as AERONET [6] is measuring AOD at standardized wavelengths (λ= 0.44, 0.67, 0.87, and 1.02 μm) all over the world. Using a logarithmic interpolation, [7], one can accurately derive AOD in a mid-visible wavelength such as λ = 0.55 μm.

Although AOD (at λ=0.55 μm) has a global mean between 0.1 and 0.15, it ranges from near zero over remote high-altitude locations to >5.0 in the path of heavy smoke plumes or dust storms. Generally, AODs > 1.0 are associated with extreme aerosol events, and values >3.0 obscure the sun's disk. AOD is inherently relevant to climate applications and direct radiative effects. Relating AOD to a mass or number concentration (including surface PM2.5) requires additional steps and assumptions [8] [9].

2. MODIS

With the launch of NASA's Terra satellite in December 1999, followed by the Aqua satellite in May 2002, our ability to characterize these small particles from space grew significantly. In particular, the MODerate resolution Imaging Spectroradiometer (MODIS) [10] and the Multi-angle Imaging SpectroRadiometer (MISR) [11] advanced passive remote sensing to quantify aerosol loading over both ocean and land, and enabled constraints on specific aerosol particle properties. MISR will be addressed in detail in a subsequent section.

MODIS is a multi-channel radiometer with 36 wavelengths spanning from 0.41 μm to 14 μm [12][13]. The breadth of MODIS's spectral range, and specifically the availability of the blue-wavelength channels (0.41 μm, 0.47 μm) and the shortwave infrared (SWIR) channels (1.2 μm, 1.6 μm and 2.1 μm) provided new capabilities for aerosol retrieval that had been unavailable from pre-2000 era predecessors such as the operational Advanced Very High Resolution Radiometer (AVHRR) [12] [13]. Additionally, technical innovations for MODIS, including on-board calibration and higher spatial resolution for some bands, fueled an ambitious research agenda to provide a robust, easy to use, global operational aerosol product. As a result, the at-launch MODIS aerosol product included many upgrades over AVHRR, including extension of aerosol optical depth (AOD) retrievals to land [14], and expansion of products over ocean to include relative aerosol size [15].

MODIS's wide-view swath (2330 km) leads to nearly global coverage each day and full Earth sampling every two days. Since there are identical MODIS instruments flying on two satellites, one on Terra with an equatorial crossing time of 10:30 Local Time and the other on Aqua with an equatorial crossing time of 13:30 Local Time, this allows full global coverage every day. The two sensors also allow for limited insight on diurnal variations from morning to afternoon [16] and can view the same geographical scene from different viewing geometries.

Figure 1 shows daily, daytime global coverage of MODIS observations from the Terra and Aqua satellites, using observed red, green and blue band observations to create "True Color" imagery. Note the different "tilt" in the orbital paths as Terra is in a daytime descending orbit and Aqua in a daytime ascending orbit, as well as the size of a 5-minute chunk of data known as a *granule*. These inclined orbits result in overpass time differences of 3 hours at the equator, 5 hours in the southern hemisphere midlatitudes and only 1.5 hours in the northern hemisphere midlatitudes.

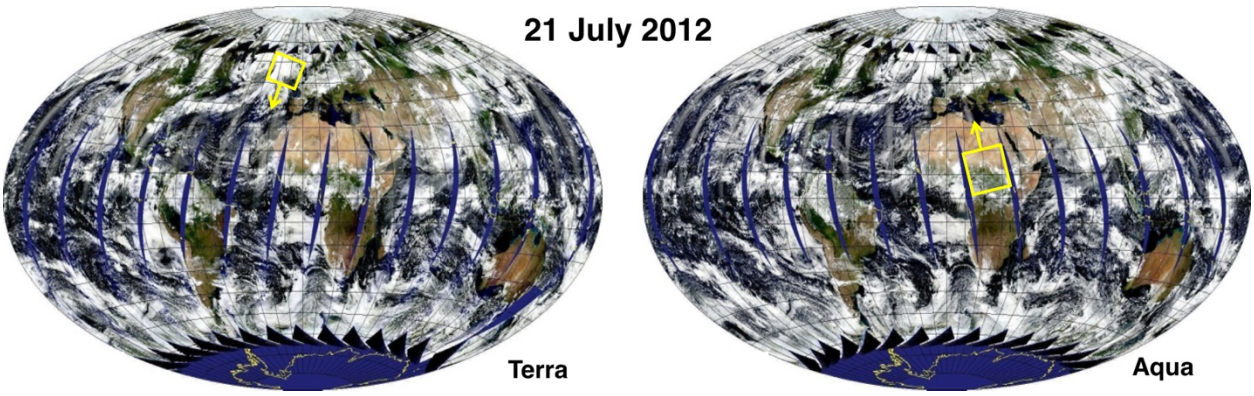

Figure 1 Example daily coverage of MODIS from Terra (left) and Aqua (right) as depicted by True-color images constructed from the red (0.65 µm), green (0.55 µm) and blue (0.47µm) measured reflectances. Yellow boxes/arrows show approximate locations of 5-minute granules and direction of flight at 12:00-12:05 UTC on 21 July 2012.

While the capabilities of the two MODIS sensors appear to allow for daily global aerosol characterization, retrieval algorithms employ conditions that limit access to the full availability of retrievals. These images illustrate the abundance of clouds, gaps between orbital swaths, glint over ocean and snow-covered land where aerosol retrievals tend to avoid. The result is that at MODIS' spatial resolution only a fraction of the original MODIS pixels are available for aerosol retrieval. In a study covering much of North America and the adjoining ocean that fraction was 34 to 43% of the total pixels [17]. Even with these limitations, the MODIS aerosol products are one of NASA's most highly used Earth Science products.

3. Aerosol Remote Sensing from MODIS

A sunphotometer directly measures the total extinction of light, leading to the AOD. The light never reaches the surface. However, MODIS, like other passive remote sensing imagers, measures the solar radiance that has been reflected or scattered. This includes scattering not only within the atmosphere (including aerosols), but also by Earth's surface. There may be multiple scatterings. The goal of aerosol remote sensing with these instruments is to infer aerosol properties from this reflected and scattered light. Therefore, to separate the aerosol signal from the other reflecting sources, there are assumptions and approximations made by the aerosol retrieval algorithms.

We present here a short summary of the theoretical basis of passive aerosol remote sensing and a subset of the important equations, following the notation used in the Algorithm Theoretical Basis Document (ATBD) of the Dark Target aerosol group [18]. We will refer to other valuable references that parallel this short summary and add context and depth.

The governing equation describing the process is given by Eq. (1).

$$\rho_\lambda^*(\theta_0,\theta,\phi) = \rho_\lambda^a(\theta_0,\theta,\phi) + \frac{T_\lambda(\theta_0)T_\lambda(\theta)\rho_\lambda^s}{1-s_\lambda\rho_\lambda^s} \qquad \text{(Eq 1)}$$

where ρ_λ^* is the *reflectance* at the top of atmosphere (TOA) measured by the sensor. The *path reflectance* ρ_λ^a is the portion of the measured reflectance that originates entirely from scattering of atmospheric constituents and never interacts with the surface. The remaining term represents the portion which has interacted with the surface. It includes the transmission through the atmosphere along the sun-surface path $T_\lambda(\theta_0)$, the transmission through the atmosphere along the surface-satellite path $T_\lambda(\theta)$, and the reflectance of the Earth's surface in the viewed pixel ρ_λ^s. The term also includes the effect of multiple scattering between the surface and atmosphere given by the denominator in the term where s_λ is the spherical albedo. The subscript, λ, indicates that the terms in the equation are wavelength dependent, and all reflectance terms are a function of viewing geometry with solar zenith θ_0, sensor view zenith angle θ and relative azimuth, ϕ. Note that reflectances are in fact the observed radiances normalized by different known factors as in the equation Eq. (2).

$$\rho_\lambda = L_\lambda \frac{\pi}{F_{0,\lambda}\cos(\theta_0)} \qquad \text{(Eq 2)}$$

Here, L_λ is the radiance normalized by the solar radiance, $F_{0,\lambda}$. Eq. (1) is illustrated schematically in Figure 2.

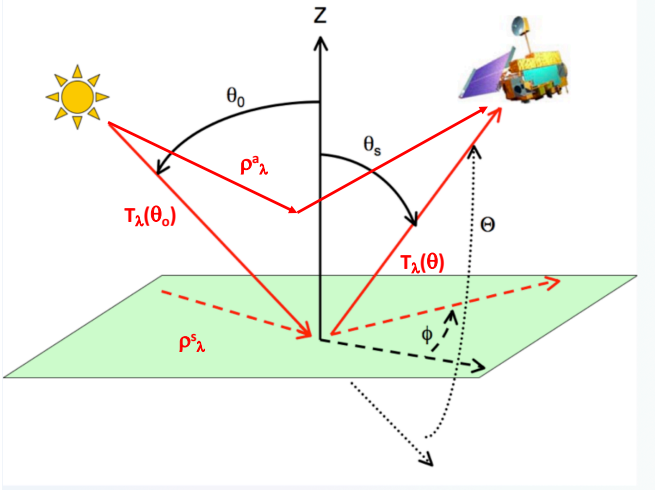

Figure 2: Schematic of the fate of reflectance that is emitted from the sun, and observed by MODIS (e.g. Equation 1), including angular definitions. Descriptions of each symbol are in the text above, except for the scattering angle (Θ).

The constituents in the atmosphere that scatter and absorb solar radiation include gas molecules, aerosols and clouds. The amount of radiance transmitted along a particular path in the atmosphere or scattered in a particular direction in a specific wavelength is determined by the amount of constituent; the size, shape and inherent optical properties of the constituent; the relative heights of the different constituents in the atmosphere; and for clouds the thermodynamic phase of the droplets/crystals.

Remote sensing is the process in reverse – using the measured spectral reflectance to infer information about the aerosol. Not all scenes are appropriate for this task. For example, clouds 'hide' the aerosol below, and bright surfaces can overwhelm the scattering signal. Therefore, to overcome instrument limitations of a passive sensor such as MODIS, several assumptions must be made. Since aerosols have spectral and angle-dependent behavior, different wavelengths and angles are better suited to observing different aerosol types. Different Earth surfaces (vegetation, deserts, water, etc.) also have their own spectral and angle-dependent behavior. We note here that there are multiple aerosol algorithms applied to MODIS and that each have strengths and weaknesses for different types of aerosols over different types of scenes.

For the standard algorithms described below, cloudy scenes will be identified a priori, and no aerosol retrieval will be attempted for those scenes. Constraining surface reflectance is key to isolating the signal to the atmosphere. Surface reflectance is assumed or estimated using long-term data bases, parameterizations or temporal consistency in an inversion that retrieves aerosol and land surface properties simultaneously. The retrieval focuses on obtaining a measure of the total amount of aerosol in the column which requires some assumptions about aerosol optical properties. Algorithms rely on pre-calculated tables that link reflectance at top-of-atmosphere to distinct levels of aerosol amount for different assumptions of aerosol optical properties at each specific wavelength and for a range of observation geometries. These pre-calculated tables are called Look Up Tables (LUT). The retrieval uses the measured TOA reflectance and searches the LUT for the specific observational geometry and assumed values for surface reflectance and aerosol optical properties to find the aerosol amount necessary to produce the measured reflectance. Thus, we infer the spectral AOD that contributed to this measurement.

3.1. Three MODIS aerosol retrieval algorithms

There are three operational MODIS aerosol retrieval algorithms. The at-launch algorithms [14] [15] is now commonly known as Dark Target or DT [19]. This was followed by the Deep Blue (DB) algorithm [20,21] and most recently by the Multi-Angle Implementation of Aerosol Correction (MAIAC) [22]. Each team has their own website with examples [[18] [23] [24]]. One should note that Dark Target and Deep Blue are maintained under the umbrella of the 'Atmosphere' discipline [25], whereas the MAIAC product is maintained under the 'Land' discipline [24]. Products from all three algorithms are publicly available.

All three retrieval algorithms use the same raw data input files. These are referred to as Level 1B (L1B) data files which include all 36 bands of calibrated radiances, along with geolocation information (latitude/longitude, observing geometry, ground-target altitude, land/sea identifier, etc.). Referring to the ground-target under the path of MODIS (nadir view), a 5-minute granule of "1 km" resolution data file is 1354 by 2030 pixels. Because MODIS is a scanning instrument, pixel size grows towards the edges of the scan, leading to the nominal "1 km" data pixel to expand to nearly 4 km at swath edge. Note that although these data are not gridded, each pixel is tagged with geolocation information.

Retrieved granule by granule, products of DT and DB have degraded resolution (N x N multiples of "1 km") and are known as Level 2 (L2). MAIAC works a bit differently, operating on aggregations of L1B known as *tiles*, leading to a gridded product (L2G) on a global grid. Data from multiple overpasses and days can be aggregated and gridded into Level 3 (L3) products.

The algorithms are similar in that they all attempt to retrieve AOD. However, they differ in 'how' they attempt to separate the atmosphere from the surface, and then the aerosol from the rest of the atmosphere. This means different choices on which scenes to select for retrieval, which wavelengths to use to perform the retrieval, and which cascading logic leads to a successful and confident derivation of AOD.

The DT algorithm was developed to derive aerosol properties over surfaces that are "dark" to our eyes. This includes vegetation and dark soils over land, as well as the deep ocean. DT produces a Level 2 AOD product in three wavelengths [14] over land and in seven wavelengths over ocean [15], with combined product defined at 0.55 μm [26] [27]. Starting by creating NxN boxes of native-resolution pixels, the algorithm screens out cloudy pixels, snow/ice, ocean glint and land surfaces with high visible and SWIR reflectance [17]. By avoiding brighter surfaces, the algorithm minimizes errors introduced by assumptions of surface reflectance. After filtering undesirable pixels, the remaining pixels in the NxN box are averaged, creating a vector of spectral reflectance that is used for the retrieval. Based on an internal land/sea flag, the algorithm will split into over-land or over-ocean. Over land, the algorithm makes use of a parameterization that connects visible to SWIR surface reflectance [[28] [27]] and assigns aerosol optical properties based on geographic regions and seasons [[29] [27]]. Over ocean, the algorithm parameterizes ocean surface reflectance as function of wind speed and allows the algorithm to choose one fine mode and one coarse mode aerosols [15] [26]. The ocean result includes a measure of particle size, in addition to the spectral AOD. The particle size parameter unique to the ocean DT algorithm is Fine Mode Fraction (FMF), which is the fraction of the total AOD (at 0.55 μm) contributed by smaller particles. This parameter supports differentiation of large particles such as dust aerosol from aerosol types dominated by smaller particle such as smoke or pollution [30][31]. The land algorithm provides a similar weighting fraction of the fine particle dominated model versus coarse particle dominated model but is considered a diagnostic of the algorithm and is not recommended for quantitative usage [27]. The standard DT products are provided at nominal 10 x 10 km resolution (at nadir), however, there is also a separate 3 x 3 km product intended for air quality applications [32] [33].

For MODIS, the DB algorithm is applied only to land pixels [20] [21] [23]. Because the fundamental gases in the atmosphere are well-mixed, their scattering is known as a function of location and surface pressure. DB uses the deviation from this well-known signature to identify the aerosol contribution to the satellite-measured reflectance [20] [21] [23]. The algorithm retrieves AOD and the spectral dependence of the AOD in the form of the Angstrom Exponent. For scenes cases identified as "dust", the single scattering albedo is also derived [21]. The algorithm is so named because it uses a "deep blue" channel at 0.41 μm, which DT does not. Molecular scattering is so strong in this wavelength that the atmospheric path reflectance ρ^a_λ dominates the measured reflectance in Eq (1). This gives the retrieval the ability to distinguish

between aerosol deviations and surface variability. Additionally, surface reflectance is naturally darker at 0.41 μm than in the mid-visible, so that the DB algorithm can make retrievals over deserts and semi-deserts, which appear bright to our eyes and to the DT algorithm [20]. The algorithm, for MODIS, is applied to cloud-free scenes, uses a LUT with assumed optical properties for smoke and dust aerosol, and bases its surface reflectance assumptions on a precalculated surface reflectance database. DB retrieval is performed on every suitable pixel, and the resulting AOD and other aerosol parameters are averaged to the same 10 x 10 km box as the standard Dark Target retrieval. The MODIS aerosol product also includes a merged DT/DB [27][34].

As mentioned above, both DT and DB operate on 5-minute granules, producing Level 2 along the orbit path. By collecting tiles that span multiple overpasses over multiple days (e.g., 8 or 16 days), the MAIAC algorithm can operate on 25 x 25 km^2 box. For this sized box on a given day, aerosol is generally much less spatially heterogenous than the land surface. However, over multiple days, the aerosol will vary much more than the land surface pattern. With the multiple viewing angles offered by 16 days of MODIS overpasses (Terra and Aqua together), MAIAC therefore can simultaneously retrieve aerosol and surface properties [22] [35]. Thus, by adding temporal information in a time series of retrieval boxes, MAIAC separates variations in measured reflectance originating from the surface from that originating from the aerosol [22]. MAIAC derives three separate products: (1) daily spectral surface reflectance, (2) daily atmospheric properties, and (3) 8-day spectral BRDF/albedo. All products are generated on a 1km sinusoidal global grid and are divided into 1200 x 1200 km^2 global tiles [22] [35]. Note that MAIAC, while being primarily an over-land algorithm, also provides retrievals over nearby water bodies.

The three algorithms are somewhat redundant, but also complement each other with different strengths. Although DT has the longest tenure on MODIS, all three algorithms have been applied to the full MODIS time series during reprocessing. DT is the only algorithm on MODIS producing aerosol properties over both land and ocean. Originally, DB extended the MODIS aerosol products to brighter surfaces, such as deserts, and now has been expanded to also retrieve over the same dark surfaces as DT. Now the L2 product includes the separate retrievals, but also a combined (merged) DT/DB AOD product [27] [34] at the 10 x 10 km resolution. The L3 product are on 1° x 1° grids and include daily, 8-day, and monthly aggregations of the separate and combined retrievals.

MAIAC is relatively new to MODIS operational processing. It sprung from the land discipline and can be found with other land discipline products [24]. Because of that, MAIAC has reduced the uncertainty in assuming land surface reflectance, and has particular strengths over difficult land surfaces, when those surfaces are invariant over the temporal averaging period. Also, because MAIAC is tiled and on a regular grid, it is not plagued by inconsistency of pixel size.

Each product has a Quality Assurance (QA) and assignment of QA Confidence, derived using a cascade of tests that follow the retrieval algorithm. Some examples of tests include counting the number of pixels used, determining the proximity to identified clouds and/or glint, and

characterizing the LUT-versus-observation fitting error. Based on these diagnostics, QAC is assigned to each successful retrieval to range from 0 (no confidence) up to 3 (high confidence). For many applications, retrievals having QAC values of 2 or 3 (medium or high) confidence are likely sufficient. For MAIAC, the QAC is reversed, such that QAC=0 refers to highest confidence.

Users should note that the three MODIS retrieval algorithms may not produce identical results over the same locations. In addition, QAC thresholds are each tied to a particular algorithm. Therefore, users must familiarize themselves with the different products to understand which is best for their particular application. See the following references which intercompare their products [34] [35].

3.2. MODIS Aerosol Products

3.2.1. Level 2 aerosol products

For DT and DB, the Level 2 (L2) retrievals are built on NxN aggregations of L1B data. DT, DB and combined DT/DB products are derived on a 10 x 10 resolution (135 x 203 pixels) and there is a DT–only retrieval at 3 x 3 resolution (451 x 676 pixels) [32] [33]. MAIAC products are different. Coming from the Land discipline, the aerosol products are organized into gridded tiles and are available at 1 km resolution at the most basic level [24].

Figure 3 shows images from Aqua MODIS on October 3, 2020 from the west coast of the United States. The true color image on the left is constructed from the measured red, green and blue reflectances. It shows a smoke plume filling California's Central Valley which is then transported out over the ocean. There are clouds offshore to the north and south. The middle three panels show Level 2 AOD products at 0.55 μm retrieved by the DT (resolution = 10x10 km^2), DB (10x10 km^2) and MAIAC (1x1 km^2) algorithms, respectively, and the right panel is the FMF retrieved by the DT algorithm. Gray areas in the product image indicate no retrieval. Filled circles overplotted on the AOD images represent observations by co-located sunphotometers (locations listed in caption).

One can see from Fig 3 both similarity and diversity of the AOD retrievals. For all images, we see cloudy areas along the coast and missing-value spots near the fire sources where the plumes are thickest. Algorithms may miss extremely thick plumes near fires because the masking routines that enable the algorithm to avoid clouds and other undesirable pixels also masks this strong, variable smoke. Although the algorithms constrain land and ocean surfaces very differently, the retrieved AOD is continuous as it transitions from land to ocean. The value of FMF ranges between 0 (all coarse-sized particles) to 1 (all fine-sized particles). In Fig.3e, the FMF is close to 1 within the smoke plume, indicating very fine particles. Farther away, FMF decreases to 0.3, which is typical of remote ocean background scenes with larger sea salt particles.

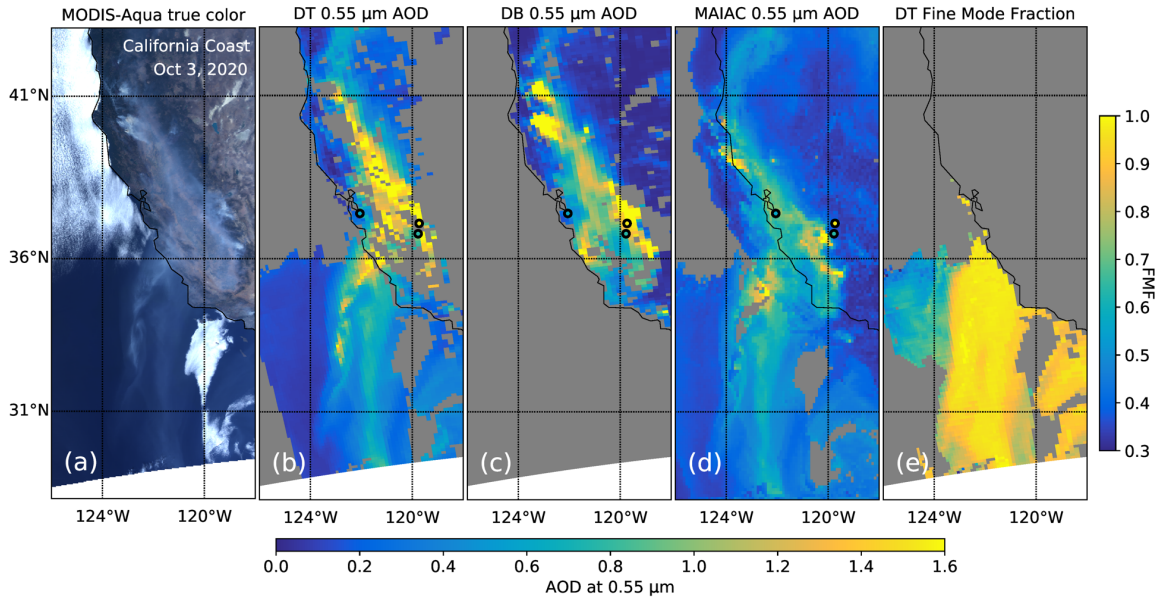

Figure 3: Illustration of MODIS Aqua image of a smoke case near California coast on October 3, 2020. (a) MODIS RGB image. Retrievals of AOD at 0.55 µm from (b) DT, (c) DB and (d) MAIAC algorithms, (e) Over-ocean AOD fine mode fraction at 0.55 µm. DT and DB retrievals are derived at non-gridded 10 km² (nadir) and are created from Aqua data only. MAIAC retrievals are derived at a gridded 1 km² and represent a combination of Terra and Aqua inputs. The tiny circles represent the AOD values reported at AERONET sites at the time of overpass. These AERONET sites include (with latitude/longitude): Fresno_2 (36.79°N, 119.77°W), NASA_Ames (37.42°N, 122.06°W) and NEON_SJER (37.11°N, 119.73°W).

3.2.2. Level 3 aerosol products

As discussed above, L2 retrievals are routinely aggregated onto a 1° x 1° grid known as Level 3 [36][37]. L3 products are available on a daily, 8-day or monthly aggregation, and data include such statistics including mean, standard deviation, minimum, maximum and pixel count for each grid box and time interval. From these standard L3 files, we can further aggregate to seasonal, annual or climatology scales.

In Figures 4 and 5, we show seasonal mean AOD and FMF at 0.55 µm, respectively, composited from the combined DT/DB products reported by MODIS from Aqua (2003-2020). Note that the aerosol size parameter (in this case FMF) is only available over the oceans. High FMF indicates aerosol dominated by small particles such as smoke and pollution. Low FMF indicates plumes dominated by large particles, mostly dust and sea salt. In this seasonal mean composite we can see the overall variability of the global aerosol system. In December-January-February (DJF), we see pollution in east Asia and northern India, along with localized dust from the African Sahel. By March-April-May (MAM), we observe active dust transport from all of the major deserts and the onset of biomass burning in southeast Asia. By June-July-August (JJA) wildfire smoke from boreal Asia and equatorial Africa have joined the active dust sources in spewing aerosol from the continents to over the ocean basins. Finally, in September-October-November (SON) the

dust sources have quieted, leaving biomass burning in the Amazon and southern Africa as the dominant aerosol regions, while pollution begins to build up again in east Asia and India.

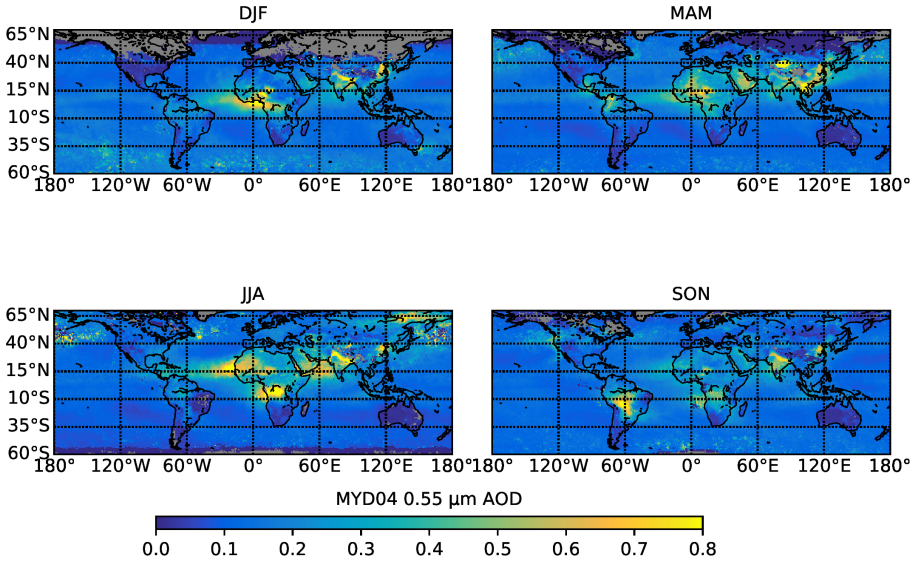

Figure 4: 1° x 1° seasonal map of AOD at 0.55 μm, calculated from the L3 monthly gridded Aqua products: 2003-2020.

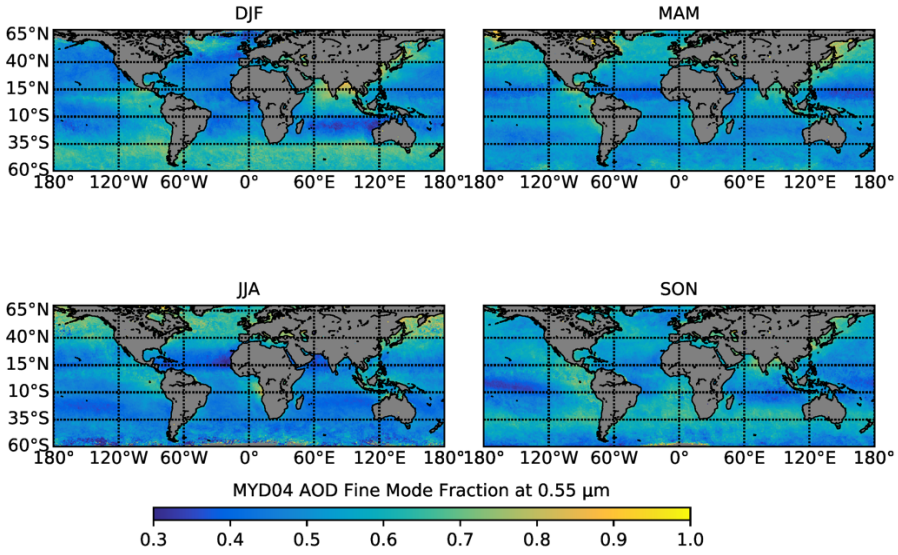

Figure 5: 1° x 1° seasonal map of FMF at 0.55 μm, calculated from the L3 monthly gridded Aqua products: 2003-2020.

Over ocean, we can combine the AOD and FMF (Dark Target algorithm) with a two-dimensional color scale, which illustrates MODIS' capability to characterize the global aerosol system. Fig. 6 (plotted for July 2008), shows intense colors to represent higher AOD, and more subdued colors

to indicate lower AOD. Reds and yellows indicate smaller particles, blue and greens show aerosol dominated by coarser particles, and light purple are the large sea salt particles. In Figure 5, we see the strong blues and greens of coarse-sized dust in the dust belt and the reds of intense biomass burning smoke in the same places seen in the JJA panel of Fig 4.

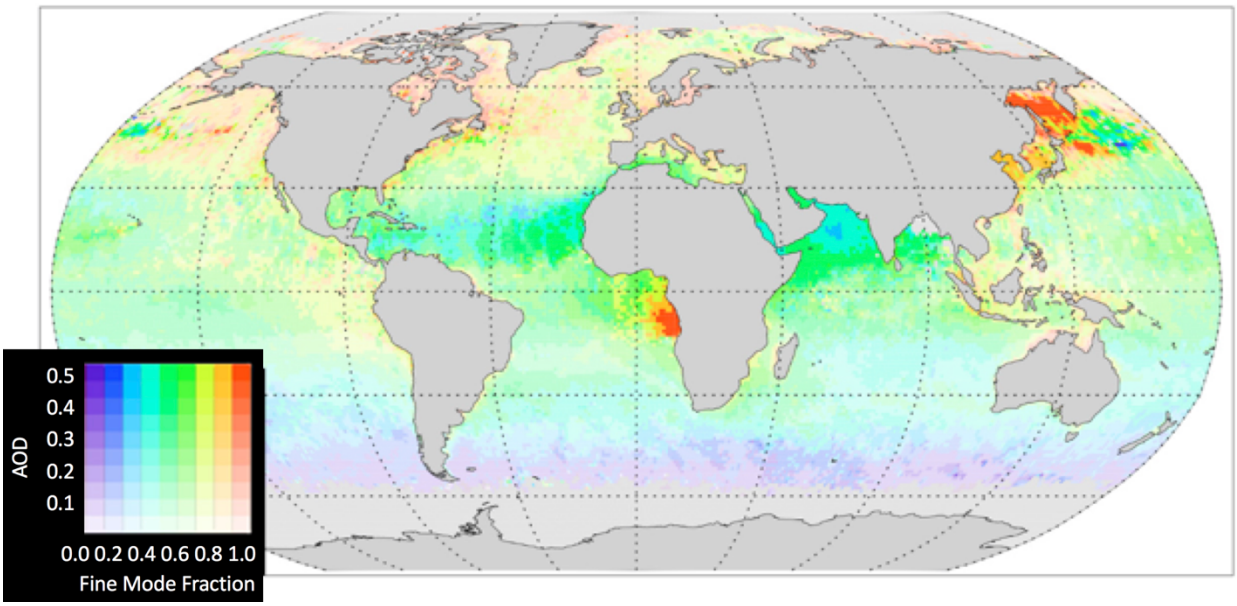

Figure 6: Monthly mean Fine Mode Fraction for July 2008. Graduations in color scale from purple to red represent changes in fine fraction from 0.0 to 1.0, respectively. Graduations in color intensity represent AOD at 0.55 μm from 0.0 to 0.80. Adapted from [8]. Reprinted with permission from Springer.

3.3. Level 2 product validation

AOD is a quantitative measure of the abundance of aerosol in the full column of the atmosphere, and a ground-based sunphotometer is theoretically the most direct method for observing AOD. Therefore, we validate our satellite retrievals of AOD by collocating with sunphotometers. The AEosol RObotic NETwork (AERONET) provides quality-assured measures of spectral AOD with well-defined uncertainties of 0.01 to 0.02 [38][39] and has been used as ground-truth by all MODIS aerosol products [13] [14] [19] [21] [22] [32] [34] [35] [40] as demonstrated in Figure 3. Figure 7 illustrates an example of statistical validation of the DT AOD product, by comparing against AERONET separately over land and over ocean. Ocean collocations are achieved from ground-based AERONET from island and coastal stations and also includes AOD measured by hand-held ship board operators of the Marine Aerosol Network [41]. Figure 7 shows the number of collocations, N, the correlation coefficient, R, the linear regression between MODIS and sunphotometer measured AOD, and the percentage of collocations falling within, above and below Expected Error (EE) as defined by previous analyses. We expect at least 67% of retrievals to fall within these error bounds. Figure 7 also shows the mean bias as a function of AERONET-measured AOD. In this example, the retrieved MODIS AOD shows essentially no bias along the full range of AOD, and the 1 standard deviation of MODIS – AERONET AOD differences are encased in the expected error bars. Similar to how

presented in [27], these data are plotted using recommended QAC filtering (≥2 over land, ≥ 1 over ocean). Note that here we are using a diagnostic description of Expected Error, where the ground-truth is presented on the X-axis.

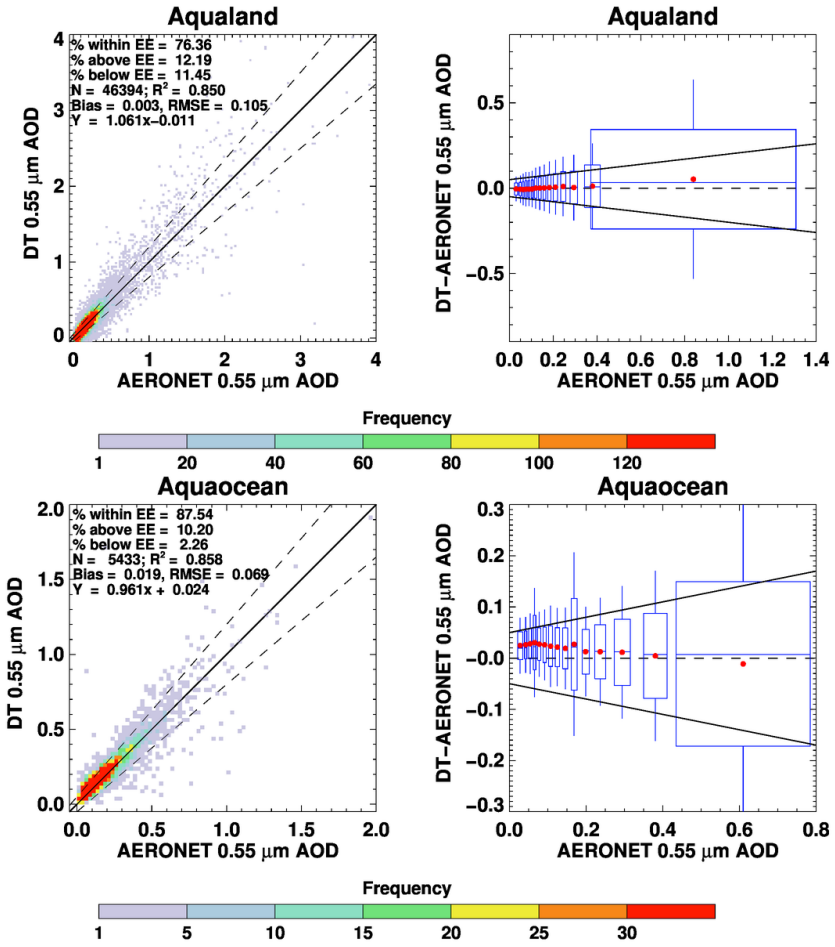

Figure 7: Left: Frequency scatter plots of DT AOD at 0.55 μm compared to the same from AERONET over land (top) and over ocean (bottom). One-one lines and expected error (EE) envelopes ±(0.05 + 15 %) are plotted as solid and dashed lines, respectively. Collocation statistics are presented in each panel. Right: the same information plotted as AOD error (MODIS-AERONET) versus AERONET AOD, broken into equal number bins of AERONET AOD for land (top) and ocean (ocean). One-one line (zero error) is dashed and EE envelopes are solid. For each box-whisker, its properties and what they represent include: width is 1-σ of the AOD bin, whereas height, whiskers, middle line and red dots are the 1-σ , 2-σ , mean and median of the AOD error, respectively. Adapted from [27].

Each MODIS aerosol team has devoted much effort to validation, using AERONET as ground truth for spectral AOD and FMF (and SSA for the DB and MAIAC algorithms), and also to confirm assumption of aerosol particle properties. Each MODIS aerosol team's web page can point the user to a list of published and unpublished validation information [18] [23] [24].

3.4. MODIS Data access

NASA maintains a series of Distributed Active Archive Centers (DAACs). Each DAAC provides multiple ways to access files, such as 1) date and area search, 2) direct access to known individual files, and/or 3) tools/instructions for creating scripts to access files. Additionally,

The DAACs will also work directly with users who need large numbers of files to establish a local archive or those who would like files pushed out to them on a regular basis.

Due to the popularity of MODIS -derived aerosol products, there are various web sites and data repositories where one can access 'value-added' products including visualizations. However, the primary archive for the DT and DB products is found at NASAs Level-1 and Atmosphere Archive & Distribution System (LAADS) DAAC [36]. The MAIAC data officially lives at the Land Processes (LP) DAAC [42] which is joint with the United States Geological Survey (USGS), but also can be found at LAADS. Recently, NASA has been creating an over-arching search and order system called EarthData [43] which includes data through Amazon Web Services. Here, we cannot provide details on how to search and download files, however there are tutorials and help files on the LAADS, LP-DAAC and EarthData sites. The NASA Applied Remote Sensing Training Program (ARSET) [44] training program also provides materials to assist with data searches.

Regardless of search location, it helps to understand data collections, file types and naming conventions. MODIS data are created and maintained in distinct *Collections*. All files in each collection will use the same set of product algorithms and apply the same calibration corrections to either the raw and/or product data. Collections have been typically updated every few years. As of this writing the MODIS DT and DB products are collection 6.1 (C61) whereas the MAIAC data are in Collection 6 (C6). Generally, only the most current collection and its immediate predecessor are available for public download.

Since there are two MODIS sensors, files from each sensor have different base naming conventions. All files from Terra begin with the name 'MOD', whereas all files from Aqua begin with 'MYD'. Files created by the combination of both are named 'MCD'. The Atmosphere-discipline aerosol products (e.g., products of DT and/or DB retrievals) are known as MxD04 (x=O or Y), with the standard 10 km Level 2 products (DT, DB, and DT/DB) denoted as MxD04_L2, and the special 3 km products (DT only) denoted as MxD04_3K. The Atmosphere-discipline Level 3 product includes aggregations of a subset of the MxD04_L2 aerosol products, bundled with a subset of products (water vapor, ozone and clouds) derived from other Atmosphere-discipline algorithms. These are known as MxD08 products and daily, eight-day, and monthly aggregations are denoted as MxD08_D3, MxD08_E3, and MxD08_M3, respectively. All standard MxD08 L3 files are at 1° x 1° latitude/longitude resolution. The MAIAC aerosol data, being created from the combination of Terra and Aqua inputs, are contained in files named MCD19A2.

The two main ways to find files are to do a search by product type, date and location (e.g. "Data Discovery" or to peruse the online directory structure to find a known file. Most users would begin with "Data Discovery", which proceeds in the following general steps:

1. Specify product type (one or more)
2. Specify time (single day/time or range of dates/times)
3. Specify location range (by latitude/longitude range, country/state shapefiles, etc.)
4. Select files (maximum of 2000 for one order)

5. Review and order files (direct download, create a script for download, etc.)

Also note that there are some advanced options that can create a more targeted search. For example, there are options to ensure deselection of night-time files (aerosol retrievals are daylight only). Advanced options will allow for selecting either cloudy or clear conditions, percentage of successful retrievals, and/or data quality. Additionally, from the LAADS website, one can select a subset of variables (post-processing) between steps 4 and 5.

3.5. Understanding and Using MODIS Aerosol Data

C6 and C61 data files are written in a heritage format known as Hierarchal Data Format version 4 (HDF4). HDF files are 'self-describing', in that metadata is included along with the data. Data variables stored in MODIS HDF files are known as Scientific Data Sets (SDSs), and each SDS includes metadata that describes its variable type (e.g., floating point, integer, byte), conversion to physical values (e.g. a slope and offset to calculate), valid-value ranges (minimum and maximum physical values), and "fill" values to represent missing data. The DT and DB Level 2 files (e.g., MxD04) as well as Level 3 (MxD08) all include many SDSs. Most SDSs are at least two-dimensional (e.g., function of X by Y) and some are three-dimensional (for example, X by Y by wavelength). It should be noted here that HDF4 is obsolete and that the "next" MODIS Collection is planned to be in Network Common Data Format version 4 (NetCDF4 [45]). There are free libraries for common programming languages including Python and Fortran. There are also free tools (see [25]).

The primary SDSs provide values at each location where the algorithm was able to complete a successful retrieval. Quality Assurance and Confidence (QAC) flag values are found in separate SDSs and are intended for filtering by expected data quality. For DT and DB, QAC flag values range from 0 to 3 (lowest to highest confidence). Assignment of QAC is a mix of objective and subjective tests that include counting the number of input pixels, deriving proximity to clouds or glint, and deriving error fitting values. Over land, values of 2 and 3 (at least medium confidence) are usually suitable for most quantitative applications, with lower values being useful for qualitative imagery and filling in gaps. Over the ocean, validation has shown that lower-confidence data can also be accurate, so that in most cases QAC≥1 is sufficient. Note that MAIAC reverses this, such that the QAC=0 indicates greatest confidence.

For the 10 x 10 km^2 MxD04_L2 granule files (DT and DB), there are in fact >75 SDSs which include latitude/longitude, altitude, angles, inputs and products of DT, DB, combined DT/DB, QAC, fitting errors, diagnostics, and further derived parameters. Key aerosol SDSs derived using DT include:

- 'Corrected_Optical_Depth_Land': AOD from DT-Land at 0.47, 0.55, and 0.65 μm, with valid range from -0.1 to 5.0. "Corrected" refers to the name of a legacy product, as there is no "Un-corrected".

- 'Optical_Depth_Ratio_Small_Land': Fraction of DT AOD contributed by the fine-dominated model for land at 0.55 μm, with valid range from 0.0 to 1.0. This SDS is to be taken as a diagnostic with limited physical application.
- 'Effective_Optical_Depth_Average_Ocean': AOD from DT-Ocean at 0.47, 0.55, 0.65, 0.86, 1.24, 1.63, and 2.11 μm. "Effective" is also a legacy name.
- 'Optical_Depth_Ratio_Small_Ocean': Ratio of Optical Depth of Small Mode to the Effective Optical Depth at 0.55 μm, with a valid range range of 0.0 to 1.0, commonly referred to as DT Fine Mode Fraction (FMF). Note there is a 3rd dimension
- 'Land_Ocean_Quality_Flag': QAC values for the DT Land and Ocean retrievals, with valid range between 0 (no confidence) and 3 (high confidence).
- 'Image_Optical_Depth_Land_And_Ocean': AOD at 0.55 μm combined from DT-Land and DT-Ocean, with no filtering for QAC. The valid range is -0.1 to 5.0
- 'Optical_Depth_Land_And_Ocean': AOD at 0.55 μm combined from DT-Land and DT-Ocean, filtered for QAC (≥2 for land, ≥1 for ocean). The valid range is -0.1 to 5.0

There are many more SDSs related to the DT aerosol retrieval (which are also in the 3 x 3 km^2 MxD04_3K granule files). Likewise, while there are many more SDSs describing DB retrieval, the following report the AOD values.

- 'Deep_Blue_Aerosol_Optical_Depth_550_Land': AOD at 0.55 μm for at-least minimal confidence (QAC ≥ 1), with valid range from 0.0 to 5.0
- 'Deep_Blue_Aerosol_Optical_Depth_550_Land_Best_Estimate' : AOD at 0.55 μm for higher quality data (QAC≥2), with valid range from 0.0 to 5.0.
- 'Deep_Blue_Aerosol_Optical_Depth_550_Land_QA_Flag' : Quality assurance (QAC) with range from 1 – 3 where one is lowest quality.

Note that while DB retrieves only physically realistic AOD values (AOD>0), DT allows for small negatives (between -0.1 and 0.0). While not valid in nature, they lead to better overall aggregate statistics. The products of the combined DT/DB retrieval include:

- 'AOD_550_Dark_Target_Deep_Blue_Combined': AOD at 0.55 μm land and ocean. DT values are used over ocean. Over land, the merge is based on climatology of NDVI, in that for lower values of NDVI, DB is chosen; for higher NDVI, DT is chosen; for medium NDVI, either the product with the higher QAC, or the average of the two [34].
- 'AOD_550_Dark_Target_Deep_Blue_Combined_Algorithm_Flag' : Flag indicating which algorithm was selected for the value of the land retrieval (0 – Dark Target, 1 – Deep Blue, 2 – Merged).
- 'AOD_550_Dark_Target_Deep_Blue_Combined_QA_Flag' : Flag indicating the QA value of the AOD retrieval in the merged product. Range is 0 – 3 where zero is low.

The Atmosphere-discipline MxD08 files are derived from aggregations of these and other aerosol SDSs, as well as SDSs from other algorithms (clouds, water vapor, atmospheric profiles, etc.). Although research has shown there is no single method for properly aggregating aerosol data, [46] laid out a methodology that is currently used. For populating a daily (MxD08_D3)

grid, there must be at least 5 aerosol retrievals (overlapping orbits are allowed), and for populating an 8-day or monthly, there must be at least 3 days represented. This reduces the possibility of having an entire month represented by a single day's retrievals, as might happen in a very cloudy location. L3 data calculations include simple statistics such as Mean, Minimum, Maximum and Standard Deviation, as well as Histograms and Pixel Counts. Additionally, for some L2 SDSs, the L3 also includes "QA Weighted" statistics, where SDSs values are weighted by their QAC values. This means that AOD values having the highest confidence (QAC=3) get 3 times the weighting of values with low confidence (QAC=1), and data with QAC=0 are ignored.

For example, the L2 SDS known as 'Corrected_Optical_Depth_Land' is reported at 0.55 μm, 0.47 and 0.65 μm. In L3, this becomes 'Aerosol_Optical_Depth_Land_STAT', noting that 'Aerosol' replaces 'Corrected' as to reduce confusing with non-aerosol variables in L3. STAT may refer to simple statistics including 'Mean', 'Standard_Deviation', 'Mininum' and 'Maximum'. STAT may also refer to 'QA_Mean' or 'QA_Standard_Deviation' which are the QAC-weighted calculations. Finally, STAT can refer to 'Histogram_Counts' (pre-defined intervals for values), or 'Confidence_Histograms' (number for each QAC value). Values at all three wavelengths are calculated. A similar set of calculations is done for the 'Effective_Optical_Depth_Ocean' (becoming 'Aerosol_Optical_Depth_Ocean_STAT'). Finally, there are statistics calculated on the pre-filtered 'Optical_Depth_Land_And_Ocean' (from DT – only), and on the pre-filtered 'AOD_550_ Dark_Target_Deep_Blue_Combined' (from DT / DB). The result is that a single grid point, there may be multiple estimates of an apparently "simple" statistic such as the Mean! There is the simple Mean (of all valid data), a QA_Mean (weighted by confidence) and the pre-filtered Mean (QAC ≥ threshold). There also may be separate retrievals from DT from DB, and from the DT/DB merge, and these daily estimates are propagated into 8-day and Monthly. The combination of all of these provides a set of uncertainty envelopes. Note that the plots in Figs 4 and 5 were calculated from aggregations of 'pre-filtered' data.

3.6. MODIS Aerosol Data Use and Air Quality Applications.

As MODIS has been in orbit on two satellites for over 20 years, there has been improvement in the sensors' calibration and aerosol retrieval algorithms. Although MODIS is a very useful sensor for characterizing AOD in ideal conditions (clear of clouds, ice, snow and glint), there is overall limited sampling (e.g., less than 10% of possible 10x10 km^2 boxes are retrieved on any given day). Even in ideal conditions, there are issues with sampling, such as skipping extremely heavy aerosol plumes (filtered out by cloud or other masking thresholds), or the opposite (thin cloud or melting snow escaping the masking thresholds). Therefore, since research has not yet determined the perfect combination of algorithms for all different conditions and applications, it is imperative that satellites retrievals are used in context with other methods for characterizing AOD and aerosol properties.

Whether one is a new or very experienced, on-line data visualizations are extremely helpful to provide context and as a "sanity check". True-color (combinations of Red-Green-Blue bands) images of each granule are available at the Atmospheric-Discipline Team Imager website [25].

These images help a user to determine if the granule corresponds to land, ocean or some mixture of the two; the degree of cloudiness, along with the likely presence of a high AOD phenomenon such as smoke, dust or a pollution event. These geo-rectified images include all granules collected since the beginning of the missions.

NASA's WorldView site [47] not only provides imagery for true-color MODIS imagery and MODIS-derived AOD retrievals, but also provides imagery for other MODIS-derived, and imagery for products from other sensors and models. All can be superimposed as "layers", and one can easily compare the different AOD retrievals from DT, DB and MAIAC, as well as with other datasets. The site provides its own extensive tutorials.

Finally, as this Handbook is about global air pollution, there is a large literature about the use of MODIS AOD products to characterize surface PM2.5. Some of the early efforts included [48] and [49], which suggested a moderate correlation between AOD and PM2.5 in many conditions. These studies have been updated, with the inclusion of meteorology and chemical transport models to include variables related to source-apportionment, vertical profiles, humidity, and other factors that impact relationships between column-integrated optical properties and surface mass concentrations. One recent example is presented by [50], which shows that a better global PM2.5 climatology arises from having multiple satellite datasets to choose from.

4. Conclusion

Aerosol algorithms applied to MODIS data have been characterizing the global aerosol system for 20 years. The products from these algorithms have supported and influenced climate prediction and processes, air quality monitoring and mitigation, data assimilation systems and our understanding of long-range transport of dust and pollutions. In addition, the algorithms developed for MODIS have provided examples for aerosol retrieval algorithms applied to other passive multi-channel satellite sensors that make observations in the solar spectrum. The MODIS example calls for a physically-based retrieval algorithm, acknowledgement of limitations, global validation using AERONET and a commitment to transparency, open data access and user support.

The three basic MODIS algorithms are in the process of being adapted to other sensors, some of which are already producing aerosol products operationally, with publicly accessible data. These include the VIsible Infrared Radiometer Suite (VIIRS) for Deep Blue [51] and Dark Target [52], and the Earth Polychromatic Imaging Camera (EPIC) for MAIAC [53]. Porting to additional sensors is an on-going effort. Of particular note is the activity to adapt these algorithms to the constellation of sensors in geostationary orbit [54]. Figure 8 shows a preliminary view of DT AOD at 0.55 μm applied to three geostationary sensors and three polar orbiting sensors at a specific time (20:45 UTC). The figure illustrates how by combining the six sensors we can enhance the coverage of Earth's global aerosol system at any particular time [19].

The MODIS aerosol algorithms developed more than 20 years ago will outlast the life time of the sensors for which they were originally designed. As such the MODIS aerosol heritage will

continue to contribute to our understanding of the Earth system, supporting air pollution and climate research, applications and policy.

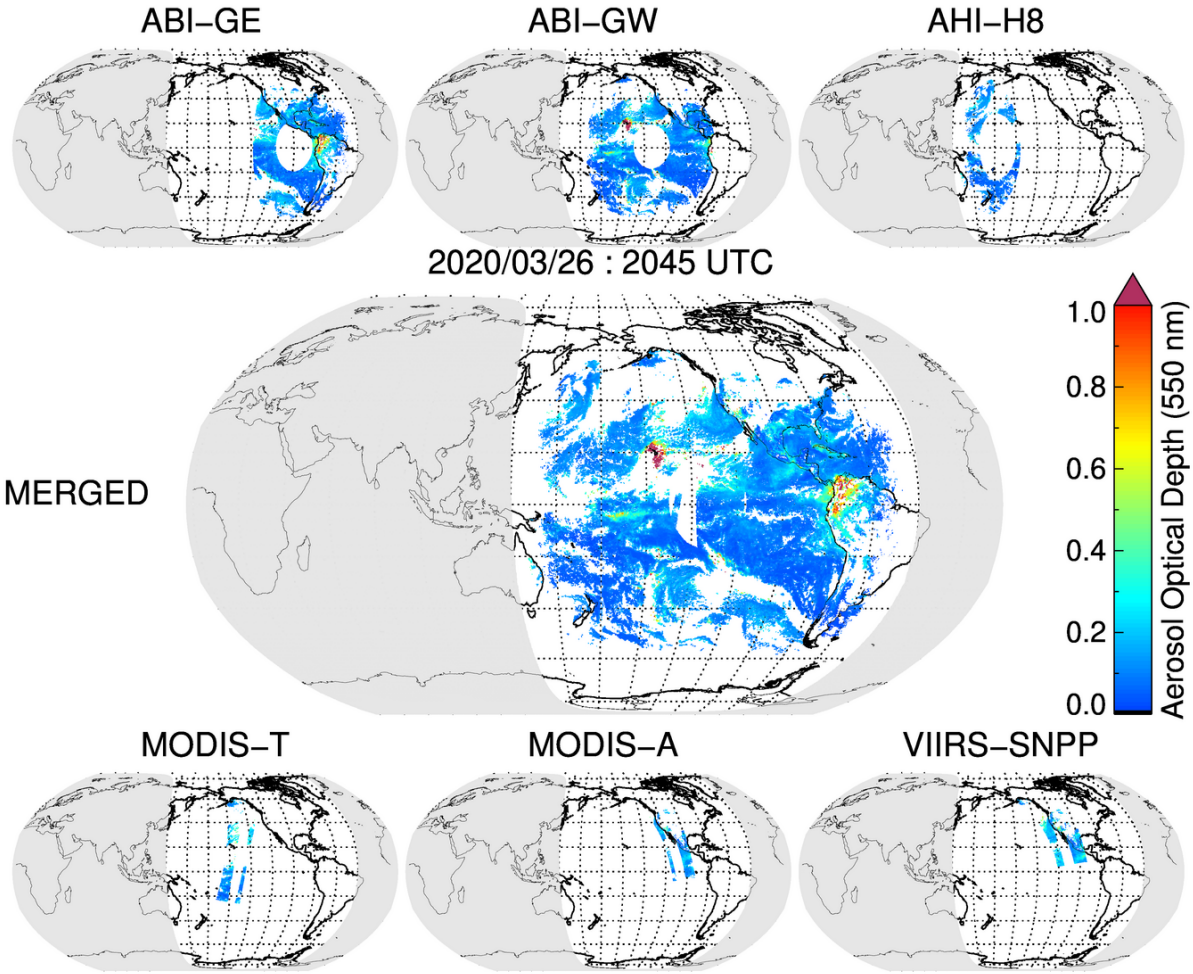

Figure 8 Aerosol optical depth at 0.55 µm, retrieved using the Dark Target aerosol algorithm with inputs from Advanced Baseline Imagers (ABIs) on GOES-E and GOES-W, Advanced Himawari Imager (AHI) on Himawari-8, MODIS on Terra and Aqua, and Visible Infrared Imaging Radiometer Suite (VIIRS) on the Suomi-National Polar-Orbiting Partnership, and the aggregated combination of the retrievals from all six sensors onto a common 0.25° by 0.25° spatial grid at 20:45 p.m. UTC ± 15 min on 26 March 2020. Gray background refers to nighttime when there are no aerosol retrievals.

Acknowledgements

This work was a "labor of love" which included participation by the entire Dark Target aerosol retrieval team. As co-authors, L. Remer, Y. Shi and R. Kleidman took the lead for text and figures while helping to consolidate contributions by P. Gupta, M. Kim, Y. Zhou, V. Sawyer and S. Gassó. Without S. Mattoo, our group's lead-programmer for 40 years, we would have no aerosol product. And without the late Yoram Kaufman, we may not have had a roadmap for creating such a product. This work was funded by NASA, currently under Senior Review (Algorithm Maintenance) support.

5. References

1. Boucher, O.; Randall, D.; Artaxo, P.; Bretherton, C.; Feingold, G.; Forster, P.; Kerminen, V.-M.;. Kondo, Y; Liao, H.; Lohmann, U.; Rasch, P.; Satheesh, S.K.; Sherwood, S.; Stevens, B.; Zhang, X.Y. Clouds and Aerosols. In: Climate Change 2013: The Physical Science Basis. Contribution of Working Group I to the *Fifth Assessment Report of the Intergovernmental Panel on Climate Change*. Stocker, T.F.; Qin, D.; Plattner, G.-K.; Tignor, M.; Allen, S.K.; Boschung, J.; Nauels, A.; Xia, Y.; Bex, V.; Midgley, P.M., Eds.,. Cambridge University Press, Cambridge, United Kingdom and New York, NY, USA. 2013.
2. IPCC, 2021: *Climate Change 2021: The Physical Science Basis. Contribution of Working Group I to the Sixth Assessment Report of the Intergovernmental Panel on Climate Change* [Masson-Delmotte, V., P. Zhai, A. Pirani, S.L. Connors, C. Péan, S. Berger, N. Caud, Y. Chen, L. Goldfarb, M.I. Gomis, M. Huang, K. Leitzell, E. Lonnoy, J.B.R. Matthews, T.K. Maycock, T. Waterfield, O. Yelekçi, R. Yu, and B. Zhou (eds.)]. Cambridge University Press. In Press.
3. Koren, I, Martins, JV, Remer, LA, Afargan, H (2008) Smoke invigoration versus inhibition of clouds over the Amazon. Science. 321: 946-949. https://doi.org/10.1126/science.1159185
4. Quaas, J, Boucher, O, Bellouin, N, Kinne, S (2008) Satellite-based estimate of the direct and indirect aerosol climate forcing. J. Geophys. Res. 113: D05204. https://doi.org/10.1029/2007JD008962.
5. McDuffie E, Martin R, Yin H, Brauer M (2021) Global Burden of Disease from Major Air Pollution Sources (GBD MAPS): A Global Approach. Research Report 210. Boston, MA: Health Effects Institute.
6. Holben BN, Eck TF, Slutsker I, Tanré D, Buis JP, Setzer A, Vermote E, Reagan JA, Kaufman Y, Nakajima T, Lavenu F, Jankowiak I, Smirnov A (1998) AERONET - A federated instrument network and data archive for aerosol characterization. Rem. Sens. Environ. 66:1-16. https://doi.org/10.1016/S0034-4257(98)00031-5
7. Eck, T. F., Holben, B. N., Reid, J. S., Dubovik, O., Smirnov, A., O'Neill, N. T., Slutsker, I., and Kinne, S. (1999), Wavelength dependence of the optical depth of biomass burning, urban, and desert dust aerosols, J. Geophys. Res., 104(D24), 31333– 31349, https://doi.org/10.1029/1999JD900923.
8. Lenoble J, Remer LA, Tanré, D (2013) Aerosol Remote Sensing. Springer Verlag Berlin Heidelberg, 390 pp., https://doi.org/10.1007/978-3-642-17725-5
9. Kokhanovsky AA, de Leeuw G (2009) Satellite Aerosol Remote Sensing Over Land. Springer, Berlin, Heidelberg. 388 pp. https://doi.org/10.1007/978-3-540-69397-0
10. https://modis.gsfc.nasa.gov/about/, accessed 18 Jan 2022
11. https://misr.jpl.nasa.gov/Mission/misrInstrument/, accessed 18 Jan 2022.
12. Salomonson, VV, Barnes, WL, Maymon, PW, Montgomery, HE, Ostrow, H (1989). MODIS – Advance facility instrument for studies of the earth as a system. IEEE Trans. Geosci. Remote Sens. 27:145-153. https://doi.org/10.1109/36.20292
13. King, MD, Kaufman, YJ, Menzel, WP, Tanré, D (1992). Remote sensing of cloud, aerosol and water vapor properties from the MODerate resolution Imaging Specrometer (MODIS). IEEE Trans. Geosci. Remote Sens. 30:2-27. https://doi.org/10.1109/36.124212
14. Kaufman, YJ, Tanré, D, Remer, LA, Vermote, E, Chu, A, Holben, BN (1997). Operational remote sensing of tropospheric aerosol over land from EOS moderate resolution imaging spectroradiometer. J. Geophys. Res., 102: 17051-17067. https://doi.org/10.1029/96JD03988.
15. Tanré, D, Kaufman YJ, Herman M, Mattoo S (1997) Remote sensing of aerosol properties over oceans using the MODIS/EOS spectral radiances. J. Geophys. Res., 102:16971– 16988. https://doi.org/10.1029/96JD03437.
16. Meskhidze N, Remer LA, Platnick S, Negrón Juárez R, Lichtenberger AM, Aiyyer AR (2009) Exploring the differences in cloud properties observed by the Terra and Aqua MODIS Sensors. Atmos. Chem. Phys. 9:3461–3475, https://doi.org/10.5194/acp-9-3461-2009.

17. Remer LA, Mattoo, S, Levy RC, Heidinger A, Pierce RB, Chin M. (2012) Retrieving aerosol in a cloudy environment: aerosol product availability as a function of spatial resolution. Atmos. Meas. Tech. 5:1823–1840, https://doi.org/10.5194/amt-5-1823-2012 .
18. https://darktarget.gsfc.nasa.gov/, accessed 18 Jan 2022.
19. Remer LA, Levy RC, Mattoo S, Tanré D, Gupta P, Shi Y, Sawyer V, Munchak LA, Zhou Y, Kim M, Ichoku C, Patadia F, Li R-R, Gassó S, Kleidman RG, Holben BN (2020) The Dark Target Algorithm for Observing the Global Aerosol System: Past, Present, and Future. Remote Sensing.12(18):2900. https://doi.org/10.3390/rs12182900
20. Hsu, N. C., Tsay, S-C, King MD, Herman J (2004) Aerosol properties over bright-reflecting source regions. IEEE Trans. Geosci. Remote Sens. 42:557– 569. https://doi.org/10.1109/TGRS.2004.824067
21. Hsu, NC, Jeong MJ, Bettenhausen C, Sayer AM, Hansell R, Seftor CS, Huang J, Tsay, S-C (2013) Enhanced Deep Blue aerosol retrieval algorithm: The second generation. J. Geophys. Res. Atmos.118:9296–9315, https://doi.org/10.1002/jgrd.50712.
22. Lyapustin A, Wang Y, Laszlo I, Kahn R, Korkin S, Remer L, Levy R, Reid JS (2011) Multiangle implementation of atmospheric correction (MAIAC): 2. Aerosol algorithm. Journal of Geophysical Research Atmospheres. 116:D03211. https://doi.org/10.1029/2010JD014986
23. https://deepblue.gsfc.nasa.gov, accessed 18 Jan 2022.
24. https://modis-land.gsfc.nasa.gov/MAIAC.html, accessed 18 Jan 2022.
25. https://atmosphere-imager.gsfc.nasa.gov, accessed 18 Jan 2022
26. Remer LA, Kaufman YJ, Tanré D, Mattoo S, Chu DA, Martins JV, Li R-R, Ichoku C, Levy RC, Kleidman RG, Eck TF, Vermote E, Holben BN (2005). The MODIS Aerosol Algorithm, Products, and Validation. Journal of the Atmospheric Sciences. 62(4), 947-973. https://doi.org/10.1175/JAS3385.1
27. Levy RC, Mattoo S, Munchak LA, Remer LA, Sayer AM, Patadia F, Hsu NC (2013)The Collection 6 MODIS aerosol products over land and ocean. Atmos. Meas. Tech., 6:2989–3034, https://doi.org/10.5194/amt-6-2989-2013.
28. Levy RC, Remer LA, Mattoo S, Vermote EF, Kaufman YJ (2007) Second-generation operational algorithm: Retrieval of aerosol properties over land from inversion of Moderate Resolution Imaging Spectroradiometer spectral reflectance. **.** J. Geophys. Res. 112:D13211. https://doi.org/10.1029/2006JD007811.
29. Levy RC, Remer LA, Dubovik O (2007) **Global aerosol optical properties and application to Moderate Resolution Imaging Spectroradiometer aerosol retrieval over land.** J. Geophys. Res. 112:D13210. https://doi.org/10.1029/2006JD007815.
30. Kaufman YJ, Boucher O, Tanré D, Chin M, Remer LA, Takemura T (2005) Aerosol anthropogenic component estimated from satellite data. Geophys. Res. Lett. 32:L17804. https://doi.org/10.1029/2005GL023125
31. Kaufman YJ, Koren I, Remer LA, Tanré D, Ginoux P, Fan S (2005) **Dust transport and deposition observed from the Terra-Moderate Resolution Imaging Spectroradiometer (MODIS) spacecraft over the Atlantic Ocean.** J. Geophys. Res. 110:D10S12, https://doi.org/10.1029/2003JD004436.
32. Remer LA, Mattoo, Levy RC, Munchak LA (2013) MODIS 3 km aerosol product: algorithm and global perspective. Atmospheric Measurement Techniques, 6 (7): 1829-1844, https://doi.org/10.5194/amt-6-1829-2013 .
33. Munchak LA, Levy RC, Mattoo S, Remer LA, Holben BN, Shafer JS, Hostetler CA, Ferrare RA (2013) MODIS 3 km aerosol product: algorithm and global perspective. Atmospheric Measurement Techniques, 6 (7): 1829-1844, https://doi.org/ 10.5194/amt-6-1829-2013 .
34. Sayer AM, Munchak LA, Hsu NC, Levy RC, Bettenhausen C, Jeong MJ (2014) MODIS Collection 6 aerosol products: Comparison between Aqua's e-Deep Blue, Dark Target, and "merged" data sets, and usage recommendations. Journal of Geophysical Research: Atmospheres, 119(24):13,965–13,989. https://doi.org/10.1002/2014JD022453.

35. Jethva H, Torres O, Yoshida Y (2019) Accuracy assessment of MODIS land aerosol optical thickness algorithms using AERONET measurements over North America. Atmospheric Measurement Techniques. 12(8):4291-4307. https://doi.org/10.5194/amt-12-4291-2019
36. https://ladsweb.modaps.eosdis.nasa.gov/missions-and-measurements/science-domain/aerosol/ (accessed 18 Jan 2022)
37. https://ladsweb.modaps.eosdis.nasa.gov/missions-and-measurements/science-domain/l3-atmosphere/ (accessed 18 Jan 2022)
38. https://aeronet.gsfc.nasa.gov (accessed 18 Jan 2022)
39. Giles DM, Sinyuk A, Sorokin MG, Schafer JS, Smirnov A, Slutsker I, Eck TF, Holben BN, Lewis JR, Campbell JR, Welton EJ, Korkin SV, Lyapustin AI (2019) Advancements in the Aerosol Robotic Network (AERONET) Version 3 database – automated near-real-time quality control algorithm with improved cloud screening for Sun photometer aerosol optical depth (AOD) measurements. Atmos. Meas. Tech. **12**:169-209. https://doi.org/10.5194/amt-12-169-2019.
40. Martins VS, Lyapustin A, de Carvalho LA, Barbosa CCF, Novo EMLDM (2017) Validation of high-resolution MAIAC aerosol product over South America. Journal of Geophysical Research: Atmospheres. 122(14):7537-7559. https://doi.org/10.1002/2016JD026301
41. Smirnov A, Holben BN, Slutsker I, Giles DM, McClain CR, Eck TF, Sakerin SM, Macke A, Croot P, Zibordi G, Quinn PK (2009) Maritime aerosol network as a component of aerosol robotic network. Journal of Geophysical Research: Atmospheres, 114:D06204, https://doi.org/10.1029/2008JD011257.
42. https://lpdaac.usgs.gov/products/mcd19a2v006/ (accessed 18 Jan 2022).
43. https://earthdata.nasa.gov/ (accessed 18 Jan 2022)
44. https://appliedsciences.nasa.gov/what-we-do/capacity-building/arset (accessed 18 Jan 2022).
45. https://www.loc.gov/preservation/digital/formats/fdd/fdd000332.shtml (accessed 18 Jan 2022).
46. Levy RC, Leptoukh G, Kahn RA, Zubko V, Gopalan A and Remer LA (2009) A Critical Look at Deriving Monthly Aerosol Optical Depth From Satellite Data. IEEE Trans. Geosci. Remote Sensing, 47 (8): 2942-2956 https://doi.org/10.1109/TGRS.2009.2013842.
47. https://worldview.earthdata.nasa.gov/ (accessed 18 Jan 2022).
48. Engel-Cox JA, Holloman CH, Coutant BW, Hoff RM. (2004) Qualitative and quantitative evaluation of MODIS satellite sensor data for regional and urban scale air quality. Atmos. Environ. 38:2495-2509. https://doi.org/10.1016/j.atmosenv.2004.01.039.
49. van Donkelaar A, Martin RV, Park RJ. (2006) **Estimating ground-level $PM_{2.5}$ using aerosol optical depth determined from satellite remote sensing.** J. Geophys. Res. 111:D21201. https://doi.org/10.1029/2005JD006996.
50. Hammer MS., van Donkelaar A, Li C, Lyapustin A, Sayer AM, Hsu N-C, Levy RC, Garay MJ, Kalashnikova OV, Kahn RA, Brauer M, Apte JS, Henze DK, Zhang L, Zhang Q, Ford B, Pierce JR, Martin RV (2020). Global Estimates and Long-Term Trends of Fine Particulate Matter Concentrations (1998–2018). Environmental Science & Technology, 54 (13): 7879-7890, https://doi.org/10.1021/acs.est.0c01764
51. Hsu NC, Lee J, Sayer AM, Kim W, Bettenhausen C, Tsay SC (2019) VIIRS Deep Blue aerosol products over land: Extending the EOS long-term aerosol data records. Journal of Geophysical Research: Atmospheres. 124(7):4026-4053. https://doi.org/10.1029/2018JD029688
52. Sawyer V, Levy RC, Mattoo S, Cureton G, Shi Y, Remer LA (2020) Continuing the MODIS Dark Target Aerosol Time Series with VIIRS. Remote Sensing 12(2):308. https://doi.org/10.3390/rs12020308 .
53. Lyapustin A, Go S, Korkin S, Wang Y, Torres O, Jethva H, Marshak A (2021) Retrievals of Aerosol Optical Depth and Spectral Absorption from DSCOVR EPIC. Frontiers in Remote Sensing 2:645794. https://doi.org/10.3389/frsen.2021.645794

54. Gupta P, Levy RC, Mattoo S, Remer LA, Holz RE, Heidinger AK (2019). Retrieval of aerosols over Asia from the Advanced Himawari Imager: Expansion of temporal coverage of the global Dark Target aerosol product. Atmospheric Measurement Techniques, 12: 6557–6577 https://doi.org/10.5194/amt-12-6557-2019